CoNTub: An Algorithm for Connecting Two Arbitrary Carbon Nanotubes

Santiago Melchor and José A. Dobado*

Grupo de Modelización y Diseño Molecular, Instituto de Biotecnología, Facultad de Ciencias, Universidad de Granada 18071, Spain

Received April 27, 2004

We have developed the first computer program for determining the coordinates of heterojunctions between two arbitrary carbon nanotubes. This software implements the topological algebra based on the concept of *strip*, a continuous subset of carbon rings containing all the topological defects (nonhexagonal carbon rings). The user easily generates any heterojunction by merely introducing the indices (*i*,*j*) and length of the two nanotubes to be connected. The resulting structure is immediately visualized and can be exported in the protein-data-bank (PDB) format. Two classes of heterojunctions are distinguished depending on whether a cone between the connected nanotubes is required. This method is applicable to all kinds of two nanotube heterojunctions, including Dunlap's knees and others related. In addition, this program also generates single- and multiwalled carbon nanotubes (SWNT and MWNT). This application has been implemented as a Java applet, and it is freely available at the following web address: http://www.ugr.es/local/gmdm/java/contub/contub.html

INTRODUCTION

Since their discovery in 1991 by Iijima,[1] carbon nanotubes have been revealed as an extraordinary material for application in multiple scientific fields, especially in electronics.[2] Apart from their striking structural properties,[3] carbon nanotubes show a special characteristic that makes them different from other materials: they are able to present metallic or semiconductor behavior depending on their geometry and the arrangement of carbon atoms. The structure of a nanotube is formed by rolling up a graphite sheet into a cylinder, being defined by the vector linking the two equivalent carbon positions that are matched together after the rolling, which is called the *chiral* vector $\boldsymbol{C}$ (see Figure 1). The decomposition of the chiral vector on the graphite-vector basis set ($\boldsymbol{a}_1$,$\boldsymbol{a}_2$) provides a pair of numbers (*i*,*j*), called the nanotube's indices.

$$\boldsymbol{C} = i\boldsymbol{a}_1 + j\boldsymbol{a}_2 \qquad (1)$$

According to the angle *Q* formed between the chiral vector and $\boldsymbol{a}_1$, nanotubes are classified as *zigzag* type (those with $j=0$ and $Q=0°$), or *armchair* type (with $i=j$ and $Q=30°$), showing higher symmetry, while the remaining nanotubes are known as *chiral*, presenting no symmetry. Hamada[4] found that carbon nanotubes, whose indices differ by a multiple of three ($i-j=3n$), show a metallic behavior, while the rest are semiconductor, with a band gap that shrinks as the nanotube radius grows.[5]

Earlier theoretical predictions[6] proposed that heterojunctions constructed with metallic and semiconductor nanotubes behave as diodes, showing highly asymmetrical (*I*/*V*) volt-ampere characteristic curves, conducting mainly in one preferred direction. Later, this was confirmed experimentally by the groups of Smalley[7] and Dekker,[8] in two remarkable experiments.[9] These experiments confirm the previous theoretical works, but the results are limited because the precise geometry of the heterojunctions remains unknown, and therefore the specific correlation between the geometry and the conductivity is not determined. Some authors postulate that the conductivity characteristics are governed only by the ratio of the connected nanotubes' diameters,[10] while others affirm that the position of pentagons and heptagons plays an important role in the conductivity properties.[11] Therefore, the geometry of the specific nanotube heterojunctions has to be clearly defined in order to progress in their research. It is common in the literature to study only relatively simple heterojunctions formed between *zigzag* and *armchair* nanotubes[8,12] or between two *zigzag* ones with different radius,[13−15] such as those shown in Figure 2, and even heterojunctions with multiple pentagonal and heptagonal rings.[6,11,16]

Nevertheless, the study of these kinds of heterojunctions raised the question as to whether it is possible to construct more of them, with a minimum number of pentagons and heptagons. The answer proved affirmative,[17,18] and moreover, it was demonstrated that the union of two nanotubes with arbitrary indices is always possible, regardless of the nanotubes' radii. Several approaches for the construction of nanotube heterojunctions have been reported[17−19] as well as an algebra to build more complex structures.[18] Given the heterojunctions formed with only a pentagon-heptagon pair, the geometry is unique. With this algoritm, it is possible to find the necessary arrangement to connect any pair of carbon nanotubes, and this underlines that the properties of a two-nanotube heterojunction structure are univocally related to the four indices of both nanotubes participating in the junction.

On the other hand, these reported methods are based on a relatively complex procedure and notation, complicating their use for construction of carbon nanostructures, and therefore

* Corresponding author phone/fax: +34 958 243186; e-mail: dobado@ugr.es.

10.1021/ci049857w CCC: $27.50
Published on Web 07/28/2004

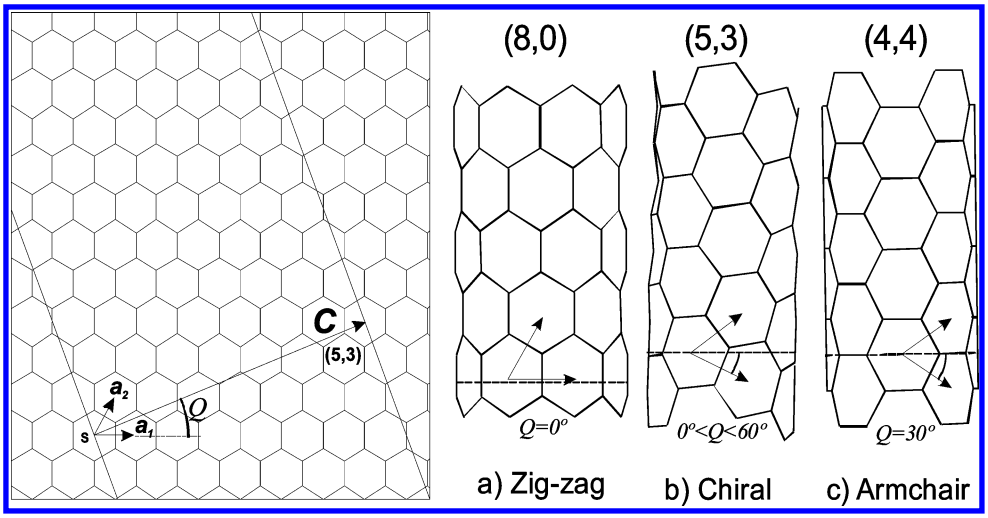

Figure 1. Definition of a nanotube's geometry by means of graphite plane rolling. Classification of a nanotube according to the *chiral* vector ***C*** and the *chiral* angle *Q* (a) *zigzag* (*i*,0); (b) *chiral* (*i*,*j*); (c) *armchair* (*i*,*i*).

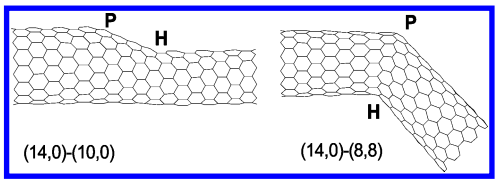

Figure 2. Nanotube heterojunctions commonly studied in the literature: (a) (14,0)−(10,0) and (b) (14,0)−(8,8). Both defects lie in the vertical symmetry plane, connecting usually *zigzag* and *armchair* nanotubes (the pentagon and heptagon are indicated with P and H, respectively).

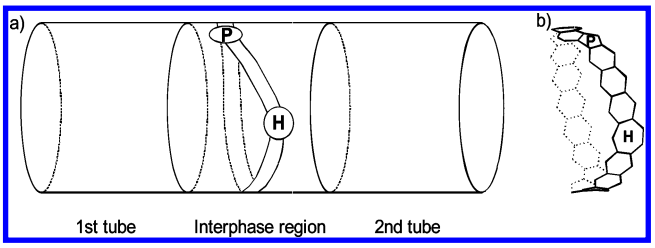

Figure 3. (a) Localization of the nonhexagonal rings within a generic nanotube heterojunction. (b) Detail of the heterojunction's *substructure* (the pentagon and heptagon are indicated with P and H, respectively).

a computational implementation became necessary. It is noteworthy that although the above-mentioned algorithms are available, studies devoted to two-tube heterojunctions are still limited to only symmetrical junctions.[6,12,14] This clearly points out the necessity of a computer program that can generate these geometries.

In principle, two nanotubes can be connected by hand, creating bonds between nonsaturated frontier atoms and adding new carbon atoms when necessary. This method can be used especially in those cases where both nanotubes have a similar symmetry and radius, as in the previously mentioned *zigzag*/*armchair* heterojunctions, where the pentagonal and heptagonal rings are placed symmetrically. The main obstacle in constructing heterojunctions by hand is the uncertainty about the positions of the pentagons and heptagons, and consequently a wrong choice forces the inclusion of other polygons (such squares or octagons), yielding highly unstable structures.

There is currently no computer application available which is able to generate the coordinates of carbon nanotube heterojunctions. This kind of software will contribute significantly to the research in the field of theoretical nanotechnology. Therefore, the main goal of the present work is the development and implementation of a general algorithm for the construction of such geometries, in an easy and efficient way, by merely introducing the indices of the nanotubes to be connected. The software accounts for the position of the defects, locates their relative orientation, and fills the remaining structure with sp^2 tricoordinated carbons. This opens the study of these complex structures to the scientific community, allowing researchers to create as many heterojunctions as required to model their properties and facilitating the understanding of these heterojunctions.

METHODOLOGY AND PROGRAMMING DETAILS

First of all, let us review the main concepts used in the determination of heterojunction geometry.[18] In a structure formed with two arbitrary nanotubes (see Figure 3), these are separated by an interphase region, composed of a set of consecutive carbon rings that encircle the tube. This belt-shaped structure, which includes the nonhexagonal rings, is called the heterojunction's substructure. Although this concept can be extended to multitube structures, for our current purpose, this is composed simply by a *strip* or path made only with hexagons and the two nonhexagonal rings, as predicted by the Euler's relationship for an infinite nanotube: N_h-$N_p = 0$ where N_p and N_h are the number of pentagons and heptagons, respectively. This path is closed over itself, in such a way that two tubes can be connected at both sides of the *strip*.

Due to the presence of just two nonhexagonal rings, the strip is divided into two units called *substrips*, each consisting of a set of contiguous hexagons and a nonhexagonal ring (see the substrip depicted in Figure 4). We arbitrarily chose to set the position of the nonhexagonal ring as the last one, in such a way that the strip is named with the position of the defect relative to the vector basis set S, located before the first hexagonal ring. To define completely the substrip as a part of the whole strip, we have to denote also how this substrip is connected to the following units. In Figure 4, the contact edges between two consecutive units are marked with

bold lines, and the vector connecting the rings of both units through the contact edges (called the exit vector) also marks the orientation of the vector basis set of the next substrip S′. The defect induces a deformation on the graphitic plane, and, therefore, there is no single orientation of the exit vector $\boldsymbol{a}_1'$ with respect to its counterpart ($\boldsymbol{a}_1$) from the original vector basis set S. Both $\boldsymbol{a}_1'$ and $\boldsymbol{a}_1$ vectors show the same orientation following a continuous path under the heptagon (dotted arrows denote intermediate orientations), but, on the other hand, following a path over the heptagon, the vector $\boldsymbol{a}_1'$ is turned −60° with respect to $\boldsymbol{a}_1$. Therefore, it is necessary to specify these orientation changes over and under the defect. We noted a strip with the indices of the defect position relative to the origin (in parentheses), and the relative orientations under and over the defect of the exit vector $\boldsymbol{a}_1'$, in 60° units (in brackets). For example, the substrip depicted in Figure 4 is noted as (3,2)[0,−1], because $\boldsymbol{a}_1'$ shows the same orientation as $\boldsymbol{a}_1$ when compared through a path under the defect but is turned −60° following a path over the defect.

As a result, the whole *strip substructure* is named with the indices and orientations of both substrip units. For convenience, we note the indices (n,m) of each strip with the initial of the defect (p or h), choosing arbitrarily the substrip containing the pentagon as the first one. Without loss of generality, a complete strip substructure, corresponding to a nanotube heterojunction constructed with a single pentagon-heptagon defect pair, is described as

$$(n_p,m_p)[0,1];\ (n_h,m_h)[0,-1] \tag{2}$$

which satisfies the condition that the sum of all turns over (and under) the strip equals 0, this being necessary to allow the connection of two tubes to the *strip substructure*. After the addition of both strips, the indices of the emerging tubes (i_1,j_1) (i_2,j_2) from the strip substructure (under and over the strip, respectively) are calculated using the following equations

$$(i_1,j_1)=(n_p,m_p) + (n_h,m_h) \tag{3.1}$$

$$(i_2,j_2) = (n_p,m_p) + O_1(n_h,m_h) \tag{3.2}$$

where $O_1(i,j)$ is an unitary operator which, given the indices (i, j) of a vector relative to the reference system S, returns the indices (i', j') in the system S′, whose basis vectors are turned 60°.

$$(i',j') = O_1(i,j) = (i + j,-i) \tag{4}$$

The process can be inverted, resulting in the method to attain the precise connectivity of two arbitrary nanotubes in the graphitic network. Furthermore, the solution always exists, and it is unique if the number of nonhexagonal rings is restricted to only one pentagon and heptagon.

$$(n_p,m_p) = (i_1 + j_1 - j_2,\ i_2 - i_1 + j_2) \tag{5.1}$$

$$(n_h,m_h) = (j_2 - j_1,\ i_1 - i_2 + j_1 - j_2) \tag{5.2}$$

The above-mentioned process is relatively complex and requires an additional understanding of the underlying principles to produce a heterojunction. Under certain conditions, these equations lead to solutions with negative indices,

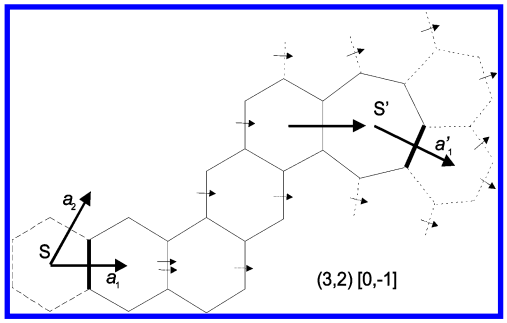

Figure 4. Detail of a *substrip* containing a heptagon. Their notation corresponds to the position of the defect with respect to the origin S and both orientations of the exit vector $\boldsymbol{a}_1'$ under (dotted small arrows) and over (solid small arrows) the defect (see text).

which are difficult to apply in a 3D structure. Therefore, it is desirable to automatize this process through a computational tool that provides the intermediate geometry for any arbitrary nanotube heterojunction, introducing just the indices of the nanotubes.

For this purpose, we have chosen the Java2 programming language. The JAVA 2 SDK,[20] Standard Edition 1.4.0_01, from Sun Microsystems is an Object-Oriented Programming language for which the main characteristics are its platform independence and ability to run in any Internet browser as an applet. An applet is a program which is downloaded from a HTML page and executed in the browser, provided that the browser supports the Java Virtual Machine (JVM). This also allows updating, so all users can work with the latest version of this software. The CoNTub program[21] has been tested for a variety of browsers and operating systems, including MS-Explorer 6.0 and Netscape 7.0.

RESULTS AND DISCUSSION

Two-Nanotube Heterojunction Construction Procedure. The construction of a nanotube heterojunction requires an additional implementation to calculate the position and connectivity of the predicted strip substructure and the rest of the structure. Once the indices of the strips are known, carbon rings should be located in the space, configuring the shape of the junction formed by the specific position of every atom present. Here, we have to deal with the deformation produced by the defects, which can be located anywhere. The presence of the nonhexagonal rings produces a curvature in the surrounding carbon network, and the shape of the connected tubes will no longer form a cylinder. As a consequence, the tubes emerging from the junction will show different orientations, and the heterojunction will present a bent shape with an angle of between 150° and 180°, the former corresponding to the Dunlap's knees.

For Dunlap's knees, the angle is the most pronounced because the pentagon and heptagon are opposed, while for the remaining junctions the bending angle is much more reduced. This is the case of the so-called "minimum curvature symmetrical knee" or Sadoc's knees,[22] where the pentagon and the heptagon form an azulene moiety in the nanotube surface. In these heterojunctions, the combination of both disclinations results in a dislocation produced by the insertion of an entire row of carbon atoms.

Nevertheless, these are only two possibilities among the multiple geometries that can be found after connecting two nanotubes. In general, a nanotube heterojunction displays no

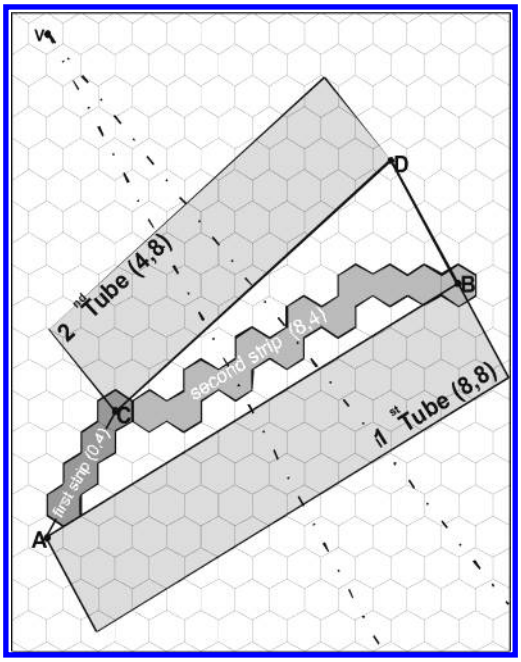

Figure 5. Projection of a (8,8)−(4,8) *cone-heterojunction* in the graphitic plane. The projected strip substructure is depicted as grayed hexagons. For clarity purposes, defect positions C and B are represented also with hexagons, although they correspond to an heptagonal and a pentagonal defect, respectively.

symmetry, and the angle formed between the two tubes is not determined. The relative orientation of both tubes emerging from the strip substructure is needed for a good atom distribution, to allow all the atoms to be equally spaced and thereby reduce the repulsion.

Therefore, the angle formed between the two tubes will depend on the relative position between the two defects, and this can be determined adequately from the strip obtained from eqs 5. The solution can be represented graphically in a graphite sheet (Figure 5), projecting in it the whole strip substructure. In the most frequent situation, the strip substructure will lie inside the polygon ACDB, where the vector AB corresponds to the chiral vector of the first tube, and CD is associated with the second tube. Both substrips marked with indices (n_p,m_p) and (n_h,m_h) resulting from eqs 5 correspond to lines CB and AC, respectively, because we have chosen that the heptagon (last ring from the first substrip in Figure 5) is located in C, while the pentagon (last ring from the second substrip) is located in A (B corresponds to its image, that after rolling the graphite sheet matches with point A).

As a result, the area contained inside the polygon ACDB has to be rolled over itself, joining the points A and C with the B and D, respectively. This forms a cone, where the sides AB and CD can hold the first and second nanotubes and V will become the vertex of that cone. Therefore, the 3D structure of these junctions will consist of the connection of the first tube, a conic section, and the second tube (see Figure 6). The dihedral angle θ formed by the pentagon and heptagon along the cone axis marks the relative orientation between the first and second tube, as the angles α_1 and α_2 next to the points *b* and *c* are independent of the dihedral θ. If $\theta = 0$, the angle between the two tubes will be a minimum of $\alpha_1-\alpha_2$, while for $\theta = 180°$, the angle will be the maximum, $\alpha_1+\alpha_2$.

Is it always possible to connect two nanotubes through a cone? The answer is no, and this can be seen in the case of an heterojunction formed by any chiral nanotube (*i*,*j*) with its mirror image (*j*,*i*). They show the same radius, and therefore the connection through a cone is not possible (see Figure 7). Consequently, we are forced to divide the heterojunctions into two classes: those formed by the combination of the first tube, a cone, and the second tube (in short, *cone-heterojunctions*) and those where the tubes involved show similar radii but different chiral angles (*radius-preserving-heterojunctions*). In terms of the projection on the graphite sheet of the strip substructure, the *radius-preserving heterojunctions* present a polygon ACDB showing a crossing between AB and CD vectors, and the second defect (C point) is located under the AB first tube chiral vector, in an area that was supposed to belong to the first nanotube. Therefore, the rolling of the planar projections of both tubes is not possible, as they superimpose themselves (dark area depicted in Figure 7).

For the *radius-preserving heterojunctions*, a different approach is needed. In Figure 7, all the defect positions are contained in the ACBD arc whose center is placed at V. This arc determines precisely the border between the first and second nanotubes, and this time there is no interphase region between both tubes. Here, the method to join the tubes consists of calculating the planar projection of both the first and second tubes, in such a way that the edges of the border coincide with the previously calculated strip substructure (eq 5). Considering the orientation reference from the first tube, we can plot the second substrip (corresponding to the line AC) and the first one (CB), as shown in Figure 8a. Therefore, the first tube is obtained after rolling the polygon $ACBB_1A_1$. This is possibly due to the previous choice of the strip denomination. In eq 2, the turn under the defects (corresponding to the first tube) is 0, so that all indices refer to the same orientation. However, the situation differs slightly for the second tube, which is located above the defects: the first substrip (C′B′ line) still shares the same orientation. The second substrip, however, appears turned 60° with respect to the first one, and therefore the AC′ line is turned 60° with respect to AC. These two lines are equivalent in the graphite network, while C′B′ and CB are parallel and indeed equivalent, and thus the dark gray polygon $AC'B'B'_2A_2$ can be turned over the light-gray one and deformed progressively (Figure 8b), until points C and C′ (and also B and B′) are joined together. This is possible because AC and BC edges are equivalent for both tubes. Once the AB and BC edges are fixed, this deformed graphitic plane can be rolled, forming a truncated cylinder (Figure 8c). Obviously, the network is highly deformed, and the generated stress has to be released appropriately in order to ensure a stable structure. This can be achieved by allowing the atoms of each tube to be redirected toward different directions, marked with two vectors, namely $\boldsymbol{n}_{T1}$ and $\boldsymbol{n}_{T2}$, corresponding to the first and second tube, respectively.

Nevertheless, the direction of these angles (and therefore, the bending angle) is undetermined. Although this angle cannot be exactly determined before the atomic distribution is known, it can be estimated considering the following:

1. Dunlap's knees, as shown in Figure 2a, are the most sharply bent junctions.

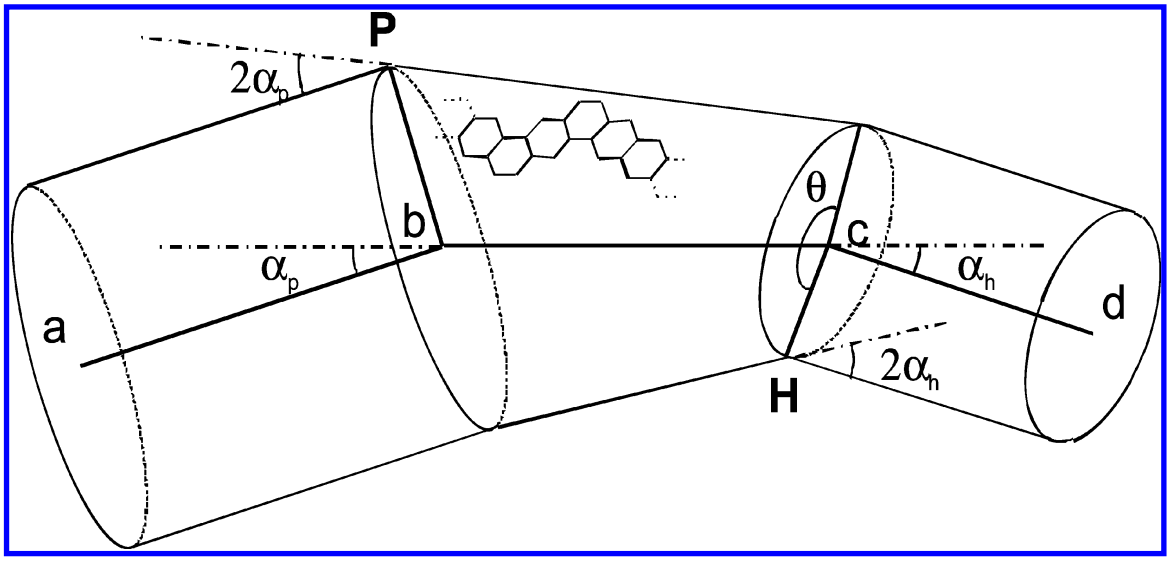

Figure 6. Heterojunction formed with a cone. The first (*ab*) and second (*cd*) tube axes subtend a dihedral angle θ with respect to the *bc* cone axis.

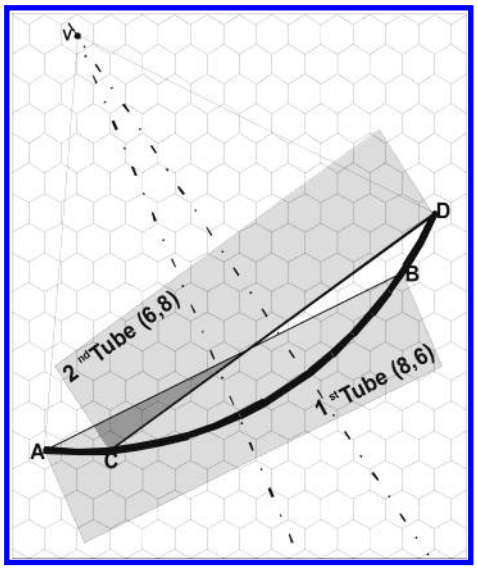

Figure 7. Projection of a *radius-preserving heterojunction* (8,6)−(6,8) in the graphite plane.

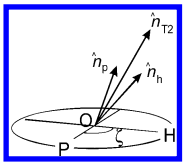

Figure 8. Stages in the building of a *radius-preserving heterojunction*. (a) Building of the polygonal sections of the graphitic plane; (b),(c) progressive deformation until ACB edges match; (d) rolling the deformed graphitic fragments to form a cylinder; (e) skewing of both tubes following the vectors $\boldsymbol{n}_{T1}$ and $\boldsymbol{n}_{T2}$.

2. Sadoc's knees, as shown in Figure 2b, present minimum curvature due to the vicinity of the two defects.

This is because the presence of a single pentagon in a cylinder makes the tube collapse progressively, displacing the area near the pentagon toward the cylinder axis, while a heptagon in a cylinder makes a wider opening, displacing the surface outward from the axis, as happens in the previous cone-heterojunctions depicted in Figure 6. The pentagon and heptagon behave oppositely, and when combined, produce a mixed geometry with a defined bending angle. As a preliminary approximation both $\boldsymbol{n}_p$ and $\boldsymbol{n}_h$ vectors, the marking of displacement induced by the pentagon and heptagon, respectively, can be added as follows:

$$\boldsymbol{n}_p = -sin(\alpha_1)\,\boldsymbol{x} + cos(\alpha_1)\,\boldsymbol{z} \tag{6.1}$$

$$\boldsymbol{n}_h = cos(\zeta)\,sin(\alpha_2)\,\boldsymbol{x} + sin(\zeta)\,sin(\alpha_2)\,\boldsymbol{y} + cos(\alpha_2)\,\boldsymbol{z} \tag{6.2}$$

where the pentagon lies on the *x* axis, ζ is the POH angle (see Figure 9) equivalent to the θ dihedral in the *cone-heterojunctions*, and α_1 and α_2 are the curvature angles corresponding to a pentagon and heptagon, respectively, as defined in Figure 6.

The result of adding the two vectors is an average direction $\boldsymbol{n}_{T2}$, which has to be followed by the second tube.

The implementation of the described algorithm generates not only Dunlap's knees or *zigzag/armchair* heterojunctions through a cone, but any other possible combination, such as *cone-heterojunctions* between chiral vectors (Figure 10a), *cone-heterojunctions* with pronounced bending angles (Figure 10b), Dunlap's knees between *chiral* nanotubes (Figure 10c), and the especially symmetrical heterojunctions between any *chiral* tube and its mirror image (Figure 10d). These heterojunctions were obtained after a single mouse click. Even more, CoNTub yields structures with enough quality to be used as an initial guess in further optimizations.

Software Description. The CoNTub program is dedicated to the construction of two nanotube junctions, but it also includes several utilities for generating straight nanotubes and performing a preliminary analysis of single nanotubes. Therefore, it is organized in three main tabbed panels to build nanotube heterojunctions, single-walled nanotubes (SWNT), and multiwalled nanotubes (MWNT), and there are also *output* and *help* sections. All panels can be used independently.

The first panel corresponds to the program core, the construction of carbon nanotube heterojunctions (see Figure 11). The use is extremely simple: the user has to introduce only the indices of the first and second tubes, the desired lengths, and to press the construction button. If desired, the open-ends of the structure can be terminated with hydrogens or nitrogens, following the Balaban[23] suggestion for obtaining

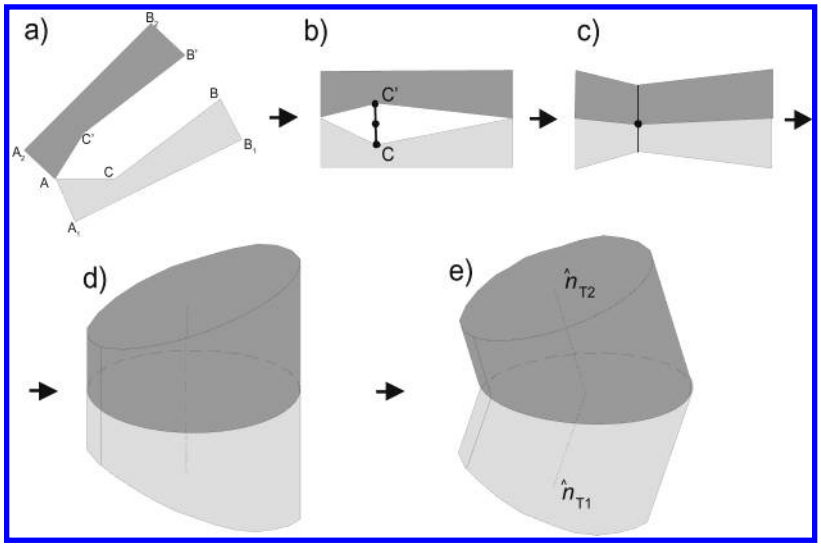

Figure 9. Second tube orientation vector, $\boldsymbol{n}_{T2}$, that results after adding the $\boldsymbol{n}_h$ and $\boldsymbol{n}_p$ vectors, depending on the position of the pentagon and the heptagon.

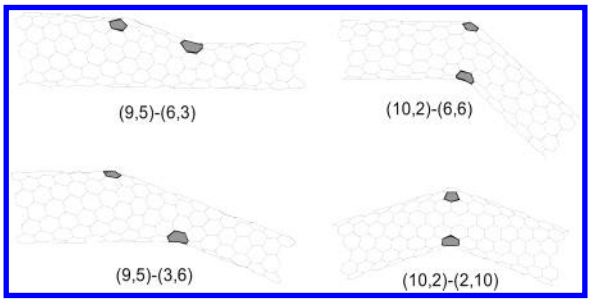

Figure 10. Structures of four different heterojunctions obtained with the CoNTub program. Shadowed polygons mark nonhexagonal rings.

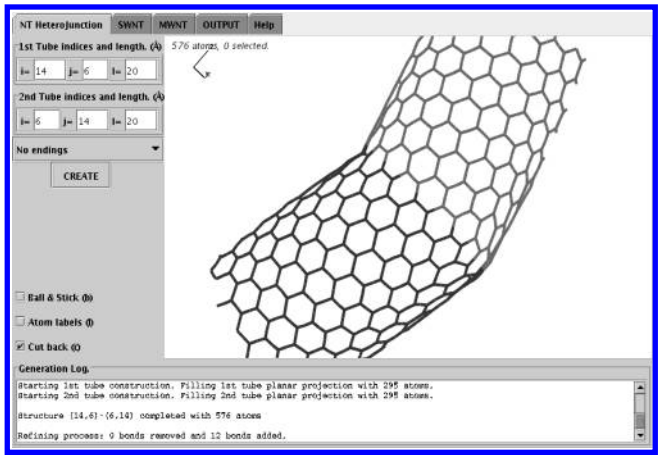

Figure 11. CoNTub's main panel for building nanotube heterostructures.

a minimum distortion at the nanotube ending. The panel is composed by a control section at the left and a 3D viewer on the right, where the heterojunction is displayed after its generation. Three additional view-switches are added: for visualizing the molecule in *ball & stick* model, for labeling the atom and for hiding the back part of the molecule (for a visualization improvement).

The user, by dragging the mouse over the display, can rotate the molecule, and by pressing the arrow keys can translate the view. Zoom is controlled with ⟨PageUp⟩ and ⟨PageDown⟩ keys. At any time the original orientation, position, and zoom can be retrieved by pressing ⟨Space⟩ key. Up to four atoms can be selected by clicking on them, and depending on the number of selected atoms, the viewer shows the following information at the bottom:

1 atom: Atom number and position.

2 atoms: Distance between atoms.

3 atoms: Angle between the last and first selected atoms, with the second atom as the vertex.

4 atoms: Dihedral angle of the last atom with respect to the first, through the line marked by the second and third selected atoms.

At any time, the atoms can be deselected by *right-clicking* on the display.

The nanotube-heterojunction building process consists of the following steps:

- Verifying the nanotube indices: The equations employed require all indices to be positive. If negative values are found, the indices are turned successively by applying the turn operator $O(i,j) = (i+j,-i)$ until both indices are positive.
- Solving the eqs 5.1 and 5.2: The strip substructure is found and reported in the log window.
- Determining of the junction type: (*cone* or *radius-preserving heterojunctions*).
- In the case of *cone-heterojunctions*, building the cone.
- Building the planar graphite fragments of both tubes.
- Determining of the orientation of the emerging tubes.
- Rolling and matching the graphite fragments.
- Detecting the connectivity between the carbon atoms.
- Finishing the dangling bonds. Figure 12 shows the Graphical User Interface (GUI) corresponding to the second panel, devoted to the conventional generation of single nanotubes, where the user chooses the indices and length of the tube. At the same time the nanotube is visualized, the band structure and density of states are displayed, following a simple tight-binding model,[24] which reveals the main electronic characteristics of the generated nanotube. In addition, the third panel generates the coordinates of MWNT's, where the user introduces the indices of the inner nanotube, its length, the number of shells composing the MWNT, and the spacing between shells. The program automatically selects tubes with the desired radius and similar chirality (unless under exceptional circumstances the coaxial nanotubes cannot display the same chirality) to generate the

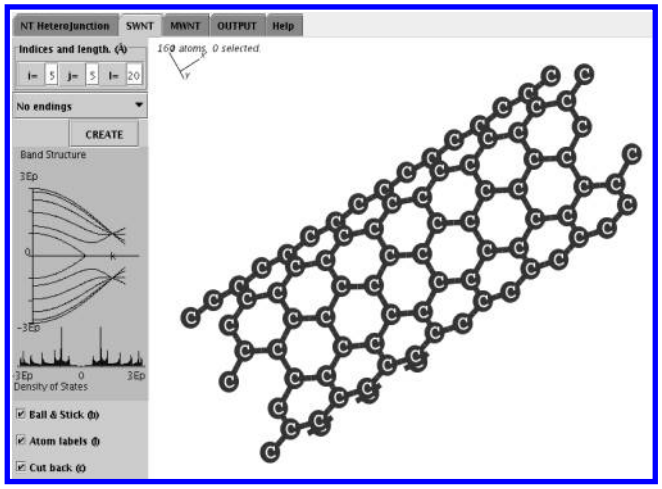

Figure 12. CoNTub's second panel for building single-walled nanotubes.

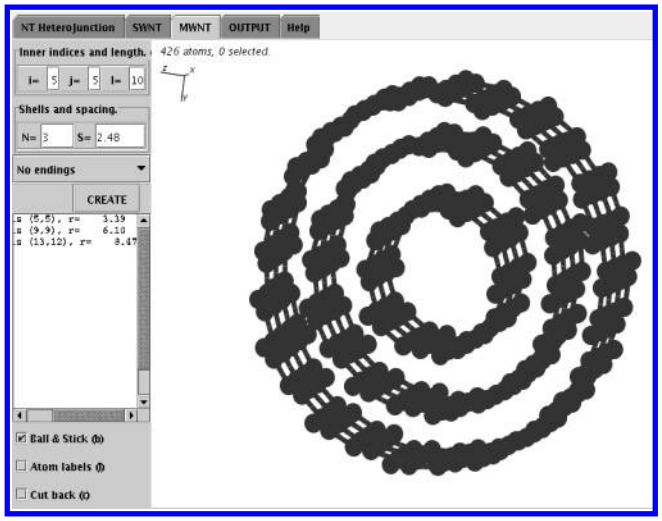

Figure 13. CoNTub's third panel for building multiwalled nanotubes.

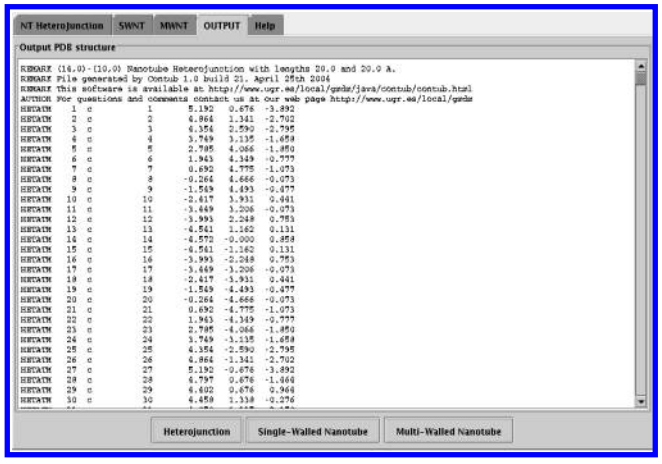

Figure 14. CoNTub's fourth panel for exporting data into PDB file format.

outer shells. Finally, all structures generated in the panels described above can be exported to the widely used Protein Data Bank (PDB) file format[25] in the fourth panel (see Figure 14). This panel consists of a text area and three buttons relative to nanotube heterojunctions, SWNT and MWNT, respectively. By pressing any of these buttons, the corresponding PDB file format is displayed in the text area, to copy and paste to the local machine.[26]

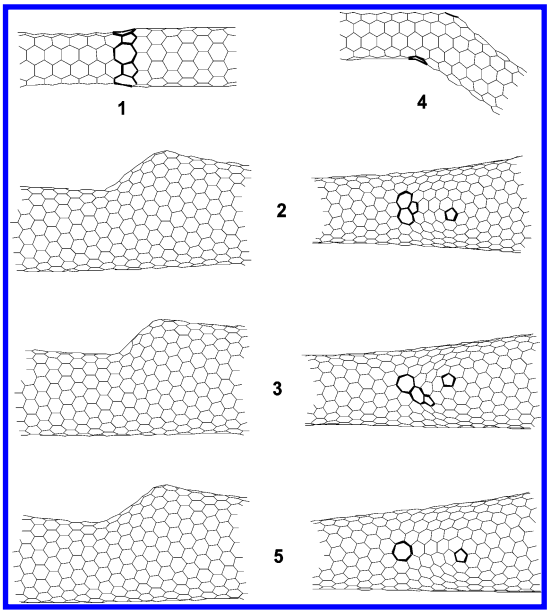

Figure 15. Nanotube heterostructures used in the literature **1**,[11] **2**[27], and **3**[16] and their equivalent alternatives **4** and **5** generated with CoNTub. Nonhexagonal rings are marked with bold lines, and heterojunctions **2**, **3**, and **5** are displayed in lateral and azimuthal views for better geometrical recognition.

Examples. One of the most important advantages of CoNTub is its ability to form nanotube structures without the specific knowledge of the interphase region. We show here three structures that have been used previously[11,16,27] in the theoretical determination of their properties. Figure 15 depicts the structures **1**−**3** from these works as well as the alternative structures **4** and **5** generated by CoNTub. The nanotube heterojunctions **1**−**3** have in common the presence of multiple pentagon-heptagon pair defects.

Structure **1**, by Treboux et al.,[11] presents a straight geometry, being characterized by five symmetrically disposed heptagon-pentagon defects, forming azulene groups. The azulene moieties appear connected consecutively forming a continuous strip, leading to a *zigzag-armchair* (10,0)−(5,5) heterojunction. On the other hand, structure **2** is an attempt to reproduce the geometry from atomically resolved scanning tunneling microscopy, obtained by Kim et al.[27] Given the chirality of both tubes, the length of the junction, and the overall shape, the authors concluded that the structure that best fit with experiment consisted in the (15,2)−(19,3) junction **2**, depicted in Figure 15. The interphase region of this structure is formed by a complex of three fused nonhexagonal rings (two heptagons and a pentagon) and an isolated pentagon. Unfortunately, the graphical representation of this work was small and ambiguous, and its precise geometrical determination was difficult to reproduce. As an indicative reference, the reconstruction of this particular (15,2)−(19,3) junction took over 3 h, because of the multiple geometrical combinations and relative orientations between the defects. Even more, a later work by Fa et al.[16] attempted to reproduce this geometry, but the resulting structure **3** is totally different from that proposed by Kim et al., because the defects are fused linearly instead of sharing a common vertex as in **2** (see Figure 15). This highlights the fact that handmade connections between tubes with known indices are often arbitrary and complex. When more than one pentagon-heptagon defect pairs are employed, the possibili-

ties are infinite, in sharp contrast with heterojunctions presenting only a pentagon-heptagon pair. In the latter case, the geometry is unique and more stable, because the number of defects is reduced to a minimum.

Structure **4**, produced with CoNTub, is the alternative heterojunction equivalent to **1**, and they differ in the overall heterojunction geometry, because structure **4** is a Dunlap's knee that shows less symmetry than **1**. Structure **5**, also generated with CoNTub, shows similar overall geometry than **2** and **3** (as can be seen in the low bending angle), but the deformation is much lower and the curvature is smoother than in **5**. Due to the higher number of defects present in **1**, **2**, and **3**, these structures are much more unstable[28] than **4** and **5** because of the deviation from the original sp^2 hybridization for each carbon atom.

CONCLUSIONS

We have described the general procedure of building three-dimensional structures of carbon nanotube heterojunctions, by simply introducing the indices of the participating nanotubes. For that purpose, we have developed and implemented this strip-based algorithm, which are defined as a continuous subset of rings containing all the non-hexagonal defects, because their relative position and orientation characterize the overall geometry and topology of the graphitic structure. According to their geometry and their building procedure, heterojunctions were classified in two categories: *cone-heterojunctions* and *radius-preserving-heterojunctions*. The former corresponds to junctions between nanotubes with different radii, and the latter to junctions preserving the radii, which include Dunlap's knees. The process described enables the study of complex and realistic carbon heterojunctions, as current investigations are limited to trivial heterojunctions with a high degree of symmetry. Furthermore, this procedure is suitable for implementation in a computer application such as CoNTub. CoNTub is a Java program that produces all types of nanotube heterojunctions connected by a single pentagon-heptagon pair. Given the indices of both nanotubes, CoNTub calculates the unique strip substructure required for the connection between the nanotubes, generates the whole heterojunction geometry, and outputs the coordinates in the Protein Data Bank (PDB) file format for further analysis. Structures generated with CoNTub (presenting only one pentagon-heptagon defect pair) have been proven to be more stable than other structures used in the literature with more defect pairs.

ACKNOWLEDGMENT

This work was supported by a project (FQM-176) financed by the *Junta de Andalucía*. Mr. David Nesbitt corrected the original English manuscript.

REFERENCES AND NOTES

(1) Iijima, S. Helical Microtubules of Graphitic Carbon. *Nature* **1991**, *354*, 56−58.
(2) Ebbesen, T. W. Carbon Nanotubes. *Phys. Today* **1996**, *49*, 26−32.
(3) Dresselhaus, M. S.; Dresselhaus, G.; Eklund, P. C. *Science of Fullerenes and Caron Nanotubes*; Academic Press: San Diego, 1995.
(4) Hamada, N.; Sawada. S.; Oshiyama, A. New One-Dimensional Conductors − Graphitic Microtubules. *Phys. Rev. Lett*. **1992**, *68*, 1579−1581.
(5) Molina, J. M.; Savinsky, S. S.; Khokhriakov, N. V. A Tight-Binding Model for Calculations of Structures and Properties of Graphitic Nanotubes. *J. Chem. Phys.* **1996**, *104*, 4652−4656.
(6) Chico, L.; Benedict, L. X.; Louie, S. G.; Cohen, M. L. Quantum Conductance of Carbon Nanotubes with Defects. *Phys. Rev. B* **1996**, *54*, 2600−2606.
(7) Collins, P. G.; Zettl, A.; Bando, H.; Thess, A.; Smalley, R. E. Nanotube Nanodevice. *Science* **1997**, *278*, 100−103.
(8) Yao, Z.; Postma, H. W. C.; Balents, L.; Dekker: C. Carbon Nanotube Intramolecular Junctions. *Nature* **1999**, *402*, 273−276.
(9) In which the nanotube heterojunctions were isolated individually, a voltage drop was applied, and the electric current through the nanotube was measured.
(10) Tamura, R.; Tsukada, M. Conductance of Nanotube Junctions and its Scaling Law. *Phys. Rev. B* **1997**, *55*, 4991−4998.
(11) Treboux, G.; Lapstun, P.; Silverbrook, K. An Intrinsic Carbon Nanotube Heterojunction Diode. *J. Phys. Chem. B* **1999**, *103*, 1871−1875.
(12) Lambin, P.; Lucas, A. A.; Charlier, J. C. Electronic Properties Of Carbon Nanotubes Containing Defects. *J. Phys. Chem. Solids* **1997**, *58*, 1833−1837.
(13) Chernozatonskii, L. A. Carbon Nanotube Connectors and Planar Jungle Gyms. *Phys. Lett. A* **1992**, *172*, 173−176.
(14) Iijima, S. Growth of Carbon Nanotubes. *Mater. Sci. Eng. B* **1993**, *19*, 172−180.
(15) Hanasaki, I.; Nakatani, A.; Kitagawa, H. Molecular Dynamics Study of Ar Flow and He Flow Inside Carbon Nanotube Junction as a Molecular Nozzle and Diffuser. *Sci. Technol. Adv. Mater.* **2004**, *5*, 107−113.
(16) Fa, W.; Yang, X.; Chen, J.; Dong, J. Optical Properties of the Semiconductor Carbon Nanotube Intramolecular Junctions. *Phys. Lett. A* **2004**, *323*, 122−131.
(17) Saito, R.; Dresselhaus, G.; Dresselhaus, M. S. Tunneling Conductance of Connected Carbon Nanotubes. *Phys. Rev. B* **1996**, *53*, 2044−2050.
(18) Melchor, S.; Khokhriakov, N. V.; Savinskii, S. S. Geometry of Multi-Tube Carbon Clusters and Electronic Transmission in Nanotube Contacts. *Mol. Eng.* **1999**, *8*, 315−344.
(19) Han, J.; Anantram, M. P.; Jaffe, R. L. Observation and Modeling of Single-Wall Carbon Nanotube Bend Junctions. *Phys. Rev. B* **1998**, *57*, 14983−14989.
(20) Sun Microsystems http://www.java.sun.com.
(21) http://www.ugr.es/local/gmdm/java/contub/contub.html.
(22) Lauginie, P.; Conard, J. *Dislocations and Other Topological Defects on Single-Walled Carbon Nanotubes;* NAMITECH. 17−21 February 1997. Valladolid, Spain.
(23) Balaban, A. T. Substitution by Heteroatoms Versus Fullerenic Capping as Remedies for Dangling Bonds in Graphene Tubulenes. *MATCH* **1996**, *33*, 25−33.
(24) Savinskii, S. S.; Khokhriakov, N. V. Characteristic Features of the π-Electron States of Carbon Nanotubes. *J. Exp. Theor. Phys.* **1997**, *84*, 1131−1137.
(25) http://www.wwpdb.org.
(26) In an effort to provide the most reliable and safe application, we have chosen not to save the files directly on the client's machine through a signed Java applet as the increasing number of computer viruses and malicious code prevents many users to allow local access to their computers. A short help and reference is given in the last panel.
(27) Kim, H.; Lee, J.; Kahng, S. J.; Son, Y. W.; Lee, S. B.; Lee, C. K.; Ihm, J.; Kuk, Y. Direct Observation of Localized Defect States in Semiconductoer Nanotube Junctions. *Phys. Rev. Lett.* **2003**, *90*, 216107.
(28) We have performed an energetical comparison between fragments of the structures reported in the literature and those generated by CoNTub, with only one pentagon-heptagon pair defect, with regular tube lengths of 12 Å, and dangling bonds filled with hydrogen atoms. For **1** and **4**, both structures showed the chemical formula $C_{260}H_{20}$, while for **2**, **3**, and **5**, the formula was $C_{657}H_{39}$. The structures were geometrically optimized with the MM+ molecular mechanics method. Structure **4** was 25.3 kcal/mol lower in energy than **1**, and structure **5** resulted in 21.2 and 58.6 kcal/mol lower than **2** and **3**, respectively.

CI049857W